Modelling Kiiking With Differential Equations

Oliver Cosgrove, Delice Mambi-Lambu, Matthew McCarthy, Aakash Datta, Jacinta Clovis, Ralph Sage

Abstract

This report aims to accurately model the sport of Kiiking by ultimately considering an anharmonic damped swing with variable length. The model is built upon the motivating case of a pendulum undergoing simple harmonic motion. Parameter dependent solutions are found using both numerical and analytical techniques, such as the fourth-order Runge-Kutta algorithm and the Phase Plane method respectively. Typical values of parameters such as height and mass of the athlete, and length and mass of the Kiiking swing are then inputted into the model in order to test its accuracy against the actual sport.

Keywords: Kiiking, Differential Equations, Runge-Kutta, Phase Planes

1 Introduction

1.1 Kiiking

Kiiking is an Estonian sport invented in the early 90s. It involves swinging on a swing with rigid arms of variable length, and trying to complete one full rotation around the swing fulcrum. The person on the swing is given an initial push, but in order to fully rotate the swing the person must manually increase the speed of the swinging via what is known as 'pumping'. This is when the person goes from a squatting to a standing position as fast as possible at the midpoint of the swing, as shown in Figure 1. It can be understood by modelling the swing as a pendulum and the person as a point mass at the end of that pendulum.

As will be shown in forthcoming sections, the maximum speed that a person can add to their rotation comes from standing up as fast as possible at the midpoint of the rotation, and then sitting down again at the maximum amplitude. The competitive nature of Kiiking comes from the fact that the natural length of the swing can be increased: more pumping is required for a longer swing to complete a full rotation, and the pumping itself on such a swing would be more physically demanding for the person.

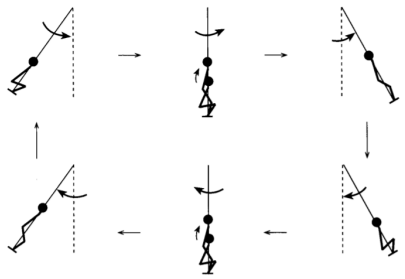

Figure 1: The motion of Kiiking or pumping a swing while standing [1].

1.2 The Models

The simplest way to model a pendulum is using simple harmonic motion (SHM). The gravitational force component is used with Newton's Second Law to find the angular acceleration. However, this model is only valid for small amplitudes as the small angle approximation is used to make the equation of motion linear in theta θ and analytically solvable.

An extension to this model does away with the small angle approx., which allows anharmonic motion to be modelled. This is the type of motion a Kiiking swing exhibits. The equation of motion becomes non-linear, so methods such as the RK4 numerical method and Phase Plane analysis are used to solve it.

The next step in improving the model comes with introducing a pendulum length that can vary in time $r(t)$. This allows for pumping to be fully incorporated in the model. The form of $r(t)$ will be a kind of continuous step function, to mimic the movement of a person going from squatting and sitting and vice versa. Finally, damping on the swing in the form of air resistance and bearing friction is considered in the model.

1.3 The Report

The evolution from model to model is outlined in section 5. Before that in section 2, the methods that will be used to solve the model are presented. In section 3, a more in-depth look into Kiiking and the physics involved in it is given. Section 4 aims to make the model as accurate as possible by addressing assumptions and providing realistic values for the parameters of the model. Finally in section 6, the results and graphs from the numerical and analytical methods are presented and discussed.

2 Methodology

2.1 Methods for Solving the Differential Equation

The Runge-Kutta method was implemented using `solve_ivp` from Python's SciPy Library and was used to solve the differential equations for modelling the motion of a Kiiking swing over time.

2.1.1 Runge-Kutta Method

The implicit Runge-Kutta method used in this model is the fourth-order (RK4) method. An increment of y is estimated using a weighted average, $k_{1\text{-}4}$. They are defined as follows [CITE ME]

$$k_1 = f(x_n, y_n) \tag{2.1}$$

This simply evaluates the Euler Approximation (see 8.8 in the appendix).

$$\begin{aligned} k_2 &= f(x_n + \frac{1}{2}h, y_n + \frac{1}{2}k_1) \\ k_3 &= f(x_n + \frac{1}{2}h, y_n + \frac{1}{2}k_2) \end{aligned} \tag{2.2}$$

These two calculate the value of x at the midpoint of the interval and therefore gives a prediction of the gradient at the prior k.

$$k_4 = f(x_n + h, y_n + k_3) \tag{2.3}$$

This computes the final point of the interval at the right side of k_3. These weights form the algorithm:

$$y_{n+1} = y_n + \frac{1}{6}(K_1 + 2K_2 + 2K_3 + K_4) \tag{2.4}$$

By incorporating the trapezoidal rule formula the Runge-Kutta method realises an increase in accuracy than that of the Euler method. Further, as shown in (2.4), k_2 and k_3 are weighted twice as much as k_1 and k_4. In combination with this, $k_{1\text{-}4}$ accounts for the whole width of the interval thus making the algorithm symmetric. This method has a local error in the 5th order ($\mathcal{O}(h^5)$) and global error in 4th order ($\mathcal{O}(h^4)$).

2.1.2 Error in Runge-Kutta Method

The step size can be made variable from the value of the truncation error. Let $y_e(x_0 + h)$ be the exact value of the solution y(x) for the initial value problem defined in (8.35) in the appendix, while the solution estimated from the Runge-Kutta method is $y_h(x_0 + h)$ [2]. From this,

$$\begin{aligned} |y_e(x_0 + h) - y_h(x_0 + h)| &= Ch^5 \\ y_e(x_0 + h) &= y_{h/2}(x_0 + h) + 2C\left(\frac{h}{2}\right)^2 \end{aligned} \tag{2.5}$$

Where C is a constant dependent on x and independent of h. Therefore the local truncation error is given by:

$$Ch^5 = \frac{y_h - y_{h/2}}{1 - 2^{-4}} \tag{2.6}$$

This implies that RK4 has high computational costs. Despite this, the implicit method is

preferable to the explicit method because its performance is not constrained by stability restrictions for local solutions at the equilibrium [3]. The tolerance used to solve each models' equations was 10^{-9}, giving a total error of 10^{-11}.

2.2 Phase Planes

The theory of phase planes can be applied to a system of non-linear autonomous differential equations where it is difficult or impossible to solve for a closed-form analytic solution using standard analytic techniques. Autonomous refers to the fact that the system cannot depend explicitly on the independent variable, t (time). One needs to first express the system in first order form:

$$\begin{aligned} du/dt &= f(u,v) \\ dv/dt &= g(u,v) \end{aligned} \tag{2.7}$$

Where u and v are functions encoding time dependence. One can say a lot about the behaviour of the analytic solution by analysing the solution trajectories in the u-v plane:

$$dv/du = g(u,v)/f(u,v) \tag{2.8}$$

The set of curves for which $\frac{dv}{du} = 0$ or ∞ are called the null clines. They divide the u-v plane into regions where $\frac{du}{dt}$ and $\frac{dv}{dt}$ are positive and negative or vice versa. The critical points are defined as the points in the u-v plane where both $\frac{dv}{dt}$ and $\frac{du}{dt}$ vanish. Critical points are only stable steady solutions to $f(u,v) = 0$ and $g(u,v) = 0$ if solution trajectories nearby tend to the point, otherwise they are unstable solutions and wont be observed in practice. To characterise the critical points, we can linearize $f(u,v)$ and $g(u,v)$ about the critical points (v_c, u_c) and then perform a Taylor series expansion to first order such that we are left with a constant coefficient system of linear ODEs, with eigenvector solutions of the form:

$$\begin{aligned} (U,V)^T &= A(\alpha_1+\beta_1)^T e^{\lambda_1 t} \\ +B(\alpha_2+\beta_2)^T e^{\lambda_2 t} &= C(dU/dt, dV/dt)^T \end{aligned} \tag{2.9}$$

The eigenvalues λ_1 and λ_2 therefore determine the solution behaviour near the critical point. If either are greater than zero in the vicinity of the critical point then the point is not stable, and wont be observed in experiment. The precise nature of a critical point can be determined by sorting the eigenvalues into 2 main categories: real or complex. In the case of real eigenvalues, the point can be shown to be either a stable node, an unstable node or a saddle (unstable). If the eigenvalues are complex conjugate pairs, then the real part of the eigenvalue pair will determine whether the point is a stable spiral, an unstable spiral or a centre (stability not well defined). This will be discussed in more detail in the results section.

Before producing a rough plot of the analytic solution in the $u-v$ plane, one must determine the symmetry of the solution about the u axis. This is straightforward if $g(u,v)$ and $f(u,v)$ are invariant under the transforms $v \to -v$, $u \to -u$ and $t \to -t$, because then the solution trajectories have reflectional symmetry across the u axis, and the phase trajectories are also closed crossing $u = 0$. In the case that the functions aren't invariant under these transforms, then one must repeat the phase-plane procedure with the new system to determine the global behaviour of the solution.

3 Theory

Kiiking is an Estonian sport in which an athlete stands on a rigid swing, which is pumped through manipulating the position of their body weight. The goal of Kiiking is to successfully complete a full revolution about the swing's fulcrum, where the winner is decided by the greatest swing arm length at which a full revolution is achieved.

In this sport, the athlete is suspended from some point by a weightful rod, about which they swing back and forth periodically. By assuming the motion of the rod, swing, and athlete are confined to a 2-D Cartesian Plane, we can treat them as one combined system and model their combined centre of mass.

The new system can be described as a Pendulum with a point mass given by the combined centre of mass, suspended from rigid support where the Swing has a negligible mass. In Kiiking, the athlete pumps the swing by transition-

ing between a sitting and squatting position at specific points. This changes the combined centre of mass of the system, allowing the athlete to increase its total angular velocity and hence progressively increase the amplitude of each swing. This change in combined of mass can be equivalently modelled by varying the Swing's length over each swing. There are two ways to account for the swing's length: Assume the length to be a constant where the constant is the average length of the swing standing and squatting, or treat the length as a variable $\mathbf{r}(t)$.

As mentioned, the motion is periodic. Hence, we define the time it takes to complete one complete oscillation as the *period* T. The amount of oscillations that occur in a unit of time is the *frequency* f where $f = 1/T$. The maximum distance that the point mass is displaced from it's equilibrium point is defined as the oscillation amplitude.

Once the Swing displaces from the equilibrium point, a restoring force will act against the direction of motion to bring the pendulum back to the equilibrium position. When the pendulum reaches and passes the equilibrium point, the restoring force changes direction towards the equilibrium point. The restoring force in the case of kiiking is friction from the pivot, drag, and the tangential component of the gravitational forces. The restoring force comes from the vector sum of the gravitational force acting on the mass, the tension and drag.

Combined, we can use Newton's Second Law for a single particle (point mass) to find the most accurate way to mathematically model the system.

3.1 Newton's Second Law

A particle acted upon by a resultant force moves in such a manner that the rate of change of it's linear momentum is equal to the resultant force.

$$\sum \underline{F} = m\underline{a} \tag{3.1}$$

For a single particle, where $\sum \underline{F}$ is the resultant force, m is the mass, and $\underline{a}$ is the acceleration.

4 Assumptions

4.1 Non-zero friction: Drag and Pivot torque

In our calculations we assume the friction to be equal to zero on the pivot. If we include pivot friction in our analysis, then the net torque on the swing at a constant length is given by:

$$\tau_N = -b\dot{\theta} - c\dot{\theta}\left|\dot{\theta}\right| \tag{4.1}$$

Where b and c are constant factors. The term that describes viscous drag which is linear in $\dot{\theta}$ is clearly much larger for all θ than the term describing friction about the pivot which is quadratic in $\dot{\theta}$, so ignoring it in our calculations is a reasonable assumption [10]. The equation of motion for our simple swing with viscous drag is given by:

$$\ddot{\theta} + \frac{C}{L}\dot{\theta} + \frac{g}{L}\sin(\theta) = 0 \tag{4.2}$$

To introduce pivot friction to the equation we define the normal force on the pivot F_N:

$$F_N = m\dot{\theta}^2 + mg\cos(\theta) \tag{4.3}$$

Assuming now that the pivot is well approximated by a spherical joint, the torque about the joint due to friction is given by:

$$\tau_p = -signum(\dot{\theta})\mu|F_N|R \tag{4.4}$$

μ is the coefficient of friction of the joint [11]. This can be anywhere between 0.5 and 0.8 for a clean, non-lubricated steel bearing, or around 0.16 for a clean lubricated steel bearing [12]. R is defined as the radius of the spherical joint. This could take a value anywhere from several cm to 10's of inches depending on the composition of the swing. Signum is a function that returns the sign of the real part of a number. This is here to ensure that the friction torque is always acting in a direction opposite to the angular velocity of the point mass.

On inclusion of the friction torque, our new equation of motion for the point mass is given by:

$$\ddot{\theta} + \frac{C}{L}\dot{\theta} + \frac{g}{L}\sin(\theta) - \frac{\tau_p}{m} = 0 \tag{4.5}$$

Which is quadratic in $\dot{\theta}$, and a small contribution compared to the other terms in the equation.

4.2 Realistic values

The platform and support rods are usually constructed from a nickel-based low-alloy steel for improved toughness and corrosion resistance [14]. The supports are assumed to be hollow, with a radius of 0.03m and a material thickness of 0.005m. The material density can be anywhere between 7.75 and 8.65 g/cm^3 depending on the ratio of nickel to pure steel. We will use the upper bound in our analysis.

We will assume the person to have a mass of 96kg, and a standing height of 1.98m. Their crouching/standing ratio will be assumed to be equal to 1/2. The length of the supports will be equal to the world-record length at 7.38m [16], however this can be varied. Finally, in our calculations we will take the decay constant $\frac{C}{L}$ to equal 0.3.

5 The Models

5.1 Motivational Model: Simple Harmonic Motion

We begin with a motivational model of using SHM for a swing. In this model, we assume that the swing is taught throughout motion for a light inextensible swing attached to a rod at one end and a point mass at the other. The swing also does not break through the motion of the swing; there is no drag and there is no friction on the pivot, and the angle of displacement from the vertical position is below $\frac{\pi}{9}$. Hence, the forces

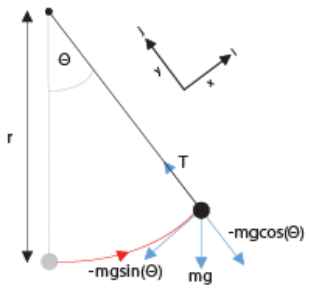

Figure 2: Free Body Diagram for SHM Model

applied are the tension, and gravity (solved in components that opposite to the tension (Normal force) and the tangential forces). Using the definition of a torque and being directly proportional to the moment of inertia we have:

$$\tau = \underline{r} \times \sum F = I\alpha \tag{5.1}$$

$$-mgsin(\theta)L = mL^2\frac{d^2\theta}{dt^2} \tag{5.2}$$

Where, $-mgsin(\theta)L$ is the torque of the restoring force and $mL^2\frac{d^2\theta}{dt^2}$ is the product of moment of inertia and the length L. Rearranging the equation produces:

$$-\frac{g}{L}sin(\theta) = \frac{\mathrm{d}^2\theta}{\mathrm{d}t^2} \tag{5.3}$$

We can Taylor expand on $sin(\theta)$ and use the fact that $|\theta| < \frac{\pi}{9}$ to justify the small angle approximation in our model.

$$sin(\theta) \approx \theta - \frac{\theta^3}{3!} + \frac{\theta^5}{5!} \approx \theta \tag{5.4}$$

Which, simplifies our equation to:

$$\frac{\mathrm{d}^2\theta}{\mathrm{d}t^2} + \frac{g}{L}\theta = 0 \tag{5.5}$$

Define, ω as $\sqrt{\frac{g}{L}}$

We, solve the Second-Order ODE to get:

$$\theta(t) = Acos(\omega t + \phi) \tag{5.6}$$

Where, A is the amplitude, t is the time, ϕ is the phase offset at t=0. The model could be a good representation of the kiiking problem as it accurately depicts how a swing would move in such a scenario. However, the model breaks down because it only works well for angular displacements $|\theta| < \frac{\pi}{9}$. Kiiking has angular displacements of $|\theta| > \frac{\pi}{9}$. Hence, the model breaks down in this case, and we don't have SHM. We have Anharmonic motion, so we have to find a more realistic model for the case of kiiking.

5.2 Model I: Anharmonic Motion Without Damping

We can describe the motion of Kiiking as Simple Anharmonic Motion. In this case, we use the same assumptions as SHM, but we also factor in the fact that the angular displacement $|\theta| > \frac{\pi}{9}$.

Hence, We cannot use the small-angle approximation, and we must use alternative methods - such as the phase-plane method for a dynamical system to solve the following ODE:

We reuse equation (5.3) and reformulate the equation defining $\frac{d\theta}{dt}$ as $\dot{\theta}$ and the definition of ω. The reformulation becomes:

$$\ddot{\theta} + \omega^2 sin(\theta) = 0 \tag{5.7}$$

We look to use the phase-plane method to solve this ODE. This is because the ODE is non-linear hence we can not use the superposition principle to solve the homogeneous ODE. Define θ as x and $\dot{\theta}$ as y we now have as a system of two coupled autonomous ODEs and look for fixed points:

$$\begin{pmatrix} x \\ y \end{pmatrix}' = \begin{pmatrix} y \\ -\omega^2 sin(x) \end{pmatrix} \tag{5.8}$$

$$(0,0)^T = (y, -\omega^2 sin(x))^T \tag{5.9}$$

Critical points $(x,y)^T$ occur at $(2n\pi,0)^T$ and $((2n+1)\pi,0)^T$ (Where $n \in \mathbb{Z}$). We seek to study the behaviour of the phase plane at our critical points, which will lead us to understand the trajectories of our phase plane. We apply the linearisation procedure to have a new system of $\hat{x}$'s and $\hat{y}$'s, thereby extracting the matrix and calculating the eigenvalues and eigenvectors for the system at the critical point, which provides us with the local analysis of the phase portrait at the points.

Linearlising at $(2n\pi,0)^T$. For $|\hat{x}| << 1$ and $|\hat{y}| << 1$. We have $(x,y)^T = (2n\pi + \hat{x}, 0 + \hat{y})^T$. Applying the addition formula and using the Taylor expansion and $|\hat{x}| << 1$:

$$\begin{aligned} sin(2n\pi + \hat{x}) &= sin(\hat{x}) \\ &\approx \hat{x} - \frac{\hat{x}^3}{3!} + \frac{\hat{x}^5}{5!} \approx \hat{x} \end{aligned} \tag{5.10}$$

The new system is under linearisation.

$$\begin{pmatrix} x \\ y \end{pmatrix}' = \begin{pmatrix} 0 & 1 \\ -\omega^2 & 0 \end{pmatrix} \begin{pmatrix} x \\ y \end{pmatrix} \tag{5.11}$$

The eigenvalues for the matrix are $\lambda_{\pm} = \pm\omega i$. Here we have imaginary roots with opposite signs and $\lambda(\mathbb{R}) = 0$. This means we have a centre where $(2n\pi,0)^T$.

Linearlising at $((2n+1)\pi,0)^T$. For $|\hat{x}| << 1$ and $|\hat{y}| << 1$. We have $(x,y)^T = ((2n+1)\pi + \hat{x}, 0 + \hat{y})^T$. Applying the addition formula and using the Taylor expansion and $|\hat{x}| << 1$:

$$\begin{aligned} sin((2n+1)\pi + \hat{x}) &= -sin(\hat{x}) \\ &\approx -\hat{x} + \frac{\hat{x}^3}{3!} - \frac{\hat{x}^5}{5!} \approx -\hat{x} \end{aligned} \tag{5.12}$$

The new system is under linearisation. .

$$\begin{pmatrix} x \\ y \end{pmatrix}' = \begin{pmatrix} 0 & 1 \\ \omega^2 & 0 \end{pmatrix} \begin{pmatrix} x \\ y \end{pmatrix} \tag{5.13}$$

The eigenvalues for the matrix are $\lambda_{\pm} = \pm\omega$. Here we have real roots with $\lambda_{-} < 0 < \lambda_{+}$; hence we have a saddle point where $((2n+1)\pi,0)^T$. We now seek to find the eigenvectors, which will give us the direction of the saddles.

For λ = ω, we have an eigenvector of $(1,\omega)^T$; for λ = -ω:, we have an eigenvector of $(1,-\omega)^T$

The appendix outlines the method of obtaining the eigenvalues and eigenvectors.

In summary, The local analysis of the model shows us that we should obtain a series of centres and saddle points at the critical points. The local analysis infers that the trajectories on the plane will focus on the critical points. However, $\frac{d\theta}{dt}$ will never converge to 0 - this means that the system will keep on running until the end of time without stopping. Furthermore, this is where **Model I** breaks as it is not able to provide an accurate outlook as we know that the existence of damping forces will cause the oscillations of the swing to diminish. However, it does allow us to account for more significant angular displacement hence better than the SHM model.

5.3 Model II: Complex Anharmonic Motion with Damping

The Model aims to focus more on being realistic by adding energy dissipation. If we assume that friction is significant in this Model, the total energy in the system is not constant, and we have E_{total} diminishing with time where each oscillation damps out. In this case, we will treat the damping force as a frictional force (drag) and

define it as being directly proportional to the angular speed where $c\frac{d\theta}{dt}$. This force acts as an additional restoring force along with the tangential component of the gravitational force. The

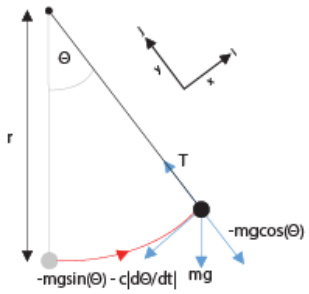

Figure 3: Free Body Diagram for Anharmonic Motion Model With Damping

model builds further on **Model I** where we use the same assumptions in the model with more of a focus on the damping of the system - the governing equation for the system (derived from Equations 5.1 and 5.3 with the addition of the damping force) .

$$\frac{\mathrm{d}^2\theta}{\mathrm{d}t^2} = -\frac{c}{L}\frac{\mathrm{d}\theta}{\mathrm{d}t} - \frac{g}{L}sin(\theta) \tag{5.14}$$

Let $\frac{c}{L} = \gamma$ and let $\omega^2 = \frac{g}{L}$ with reformulation we have:

$$\theta'' + \gamma\theta' + \omega^2 sin(\theta) = 0 \tag{5.15}$$

We repeat finding phase plane solutions due to having a non-linear homogenous ODE. Define θ as x and $\frac{d\theta}{dt}$ as y, and we create a system of two coupled autonomous ODEs and look for critical points.

$$\begin{pmatrix} x \\ y \end{pmatrix}' = \begin{pmatrix} y \\ -\omega^2 sin(x) - \gamma y \end{pmatrix} \tag{5.16}$$

$$(0,0)^T = (y, -\omega^2 sin(x))^T \tag{5.17}$$

Critical points $(x,y)^T$ occur at $(2n\pi,0)^T$ and $((2n+1)\pi,0)^T$ (Where $n \in \mathbb{Z}$).

We seek to analyse the local behaviour of the phase plane at these critical points. Therefore, implying the trajectories that stem from the points. We repeat the linearisation process and extract a matrix to find its eigenvalues and eigenvectors.

Linearlising at $(2n\pi,0)^T$. We have $(x,y)^T = (2n\pi + \hat{x}, 0 + \hat{y})^T$. For $|\hat{x}| << 1$ and $|\hat{y}| << 1$. Following from equation (5.11). We get a new system under linearlisation.

$$\begin{pmatrix} x \\ y \end{pmatrix}' = \begin{pmatrix} 0 & 1 \\ -\omega^2 & -\gamma \end{pmatrix} \begin{pmatrix} x \\ y \end{pmatrix} \tag{5.18}$$

The eigenvalues for the matrix are

$$\lambda_{\pm} = -\frac{\gamma}{2} \pm i\sqrt{\omega^2 - \frac{\gamma^2}{4}}$$

Here we have complex roots where the $\lambda(\mathbb{R}) < 0$. Hence, we have a stable spiral at the points $((2n+1)\pi,0)^T$.

Linearlising at $((2n+1)\pi,0)^T$. We have $(x,y)^T = ((2n+1)\pi + \hat{x}, 0 + \hat{y})^T$. For $|\hat{x}| << 1$ and $|\hat{y}| << 1$. Following from equation (5.13). We get a new system under linearlisation.

$$\begin{pmatrix} x \\ y \end{pmatrix}' = \begin{pmatrix} 0 & 1 \\ \omega^2 & -\gamma \end{pmatrix} \begin{pmatrix} x \\ y \end{pmatrix} \tag{5.19}$$

The eigenvalues for the matrix are

$$\lambda_{\pm} = -\frac{\gamma}{2} \pm \sqrt{\omega^2 + \frac{\gamma^2}{4}}$$

Here we have real roots with $\lambda_- < 0 < \lambda_+$. This means we have a Saddle point at the points $((2n+1)\pi,0)^T$.

The appendix outlines the method of obtaining the eigenvalues and eigenvectors.

In Summary, the local analysis of the critical points shows that we have a series of saddle points and stable spirals. The local analysis infers that the trajectories on the plane will focus on the critical points. In this case, The trajectories will lead to $\frac{d\theta}{dt}$ to diminish to 0; this is due to the existence of stable spirals, which means that the trajectories will focus inwards towards the Even critical points. Inferring, whilst the athlete can achieve a full cycle, eventually, the angular velocity will converge to 0. In comparison to **Model I** where the existence of centres show that the system will continue to run as t tends to ∞. **Model II** provides a more realistic outlook on the motion of kiiking as it shows the

process the athlete undergoes to gain amplitude; then, once the athlete reaches maximum amplitude, the athlete energy will eventually dissipate, leading the angular velocity to tend to 0.

The Model breaks down as it cannot account for the variable length of the swing and the ways energy could be lost as we only focus on drag and tangential gravity as the only restoring forces. In the next Model, we will look at how the change of centre of mass can influence how our governing equations change

5.4 Model III: Anharmonic Motion with variable $r(t)$ and No Damping

Taking the polar co-ordinates derived in appendix section 8.10, resolving the $\mathbf{e}_r$ component of equation 8.52 vector equation leads to an ODE for $\theta(t)$:

$$2\dot{r}\dot{\theta} + r\ddot{\theta} = -g\sin\theta \tag{5.20}$$

If we impose that r can only depend on θ and $\dot{\theta}$, then equation 5.20 can be converted from one second-order equation into a system of two first-order equations using the substitution:

$$\dot{\theta} = d\theta/dt = u \tag{5.21}$$

$$\ddot{\theta} = du/dt = -\frac{1}{r}(g\sin\theta + 2u\dot{r}) \tag{5.22}$$

The above system of coupled differential equations can now be solved numerically using `solve_ivp`, once the form of $r(\theta,\dot{\theta})$ and $\dot{r}(\theta,\dot{\theta})$ has been determined.

5.4.1 Pumping from Standing Position

Assuming a person is stood on the swing, in the same plane as the poles, they can be approximated as a point mass at the location of their centre of mass. Then the pumping motion can be approximated as a change in length of the pole as the centre of mass moves up and down. Assuming this pump motion is instantaneous we need to use a step function to approximate r. Using $tanh$ to approximate a step function we find:

$$r = -a\frac{\dot{\theta}}{|\dot{\theta}|}tanh(1000\cdot\theta) + b \tag{5.23}$$

Where $a = \frac{\Delta L}{2}$ and $b = \frac{L_{standing}-\Delta L}{2}$, the 1000 factor included in the tanh function is there to make the change instantaneous and ensure r imitates a step function. Figure 4 shows equation 5.23 plotted indicating how with $+\theta,+\dot{\theta}$ and $-\theta,-\dot{\theta}$ the length is longer (the person is crouched) and with $-\theta,+\dot{\theta}$ and $+\theta,-\dot{\theta}$ the length is shorter (the person is standing).

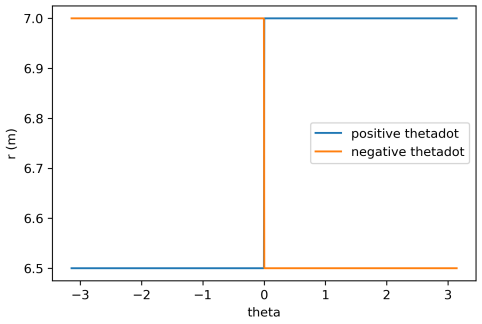

Figure 4: plot of equation 5.23 showcasing how r changes as the swing is pumped

Then in order to subsitute this function into equation 8.47 we need to find $\dot{r}$, by differentiating equation 5.23 we find:

$$\begin{aligned}\dot{r} &= -a\left[\ddot{\theta}\frac{1}{|\dot{\theta}|}tanh(1000\theta)\right.\\ &- \frac{\dot{\theta}\ddot{\theta}}{|\dot{\theta}|^3}\dot{\theta}tanh(1000\theta)\\ &\left.+ 1000\cdot\dot{\theta}sech^2(1000\theta)\frac{\dot{\theta}}{|\dot{\theta}|}\right]\end{aligned} \tag{5.24}$$

Then both r and $\dot{r}$ can be subsitutued into equation 8.47 to find:

$$\begin{aligned}&-2a\dot{\theta}\left[\frac{\ddot{\theta}}{|\dot{\theta}|}tanh(1000\theta)\right.\\ &- \frac{\dot{\theta}^2\ddot{\theta}}{|\dot{\theta}|^3}tanh(1000\theta)\\ &\left.+ 1000\cdot sech^2(1000\theta)\frac{\dot{\theta}^2}{|\dot{\theta}|}\right]\\ &- a\frac{\ddot{\theta}\dot{\theta}}{|\dot{\theta}|}tanh(1000\theta) + \ddot{\theta}b = -gsin(\theta)\end{aligned} \tag{5.25}$$

This can then be simplified to:

$$\ddot{\theta} = \frac{-gsin(\theta) + 2000a\frac{\dot{\theta}^3}{|\dot{\theta}|}sech^2(1000\theta)}{2a\frac{\dot{\theta}}{|\dot{\theta}|}tanh(1000\theta)\left[\frac{\dot{\theta}}{|\dot{\theta}|^2} - \frac{3}{2}\right] + b} \tag{5.26}$$

This is the 2nd order differential equation which we need to solve. First using the 1st order reduction outlined in section 5.4 and then applying `solve_ivp`.

6 Results and Discussion

Some assumptions of our model have been discussed already, but we will list them here explicitly:

1. The Kiiking swing supports are light, rigid and inextensible. This entails that the rods attached to the seat of the swing about which it rotates stay taught at large amplitudes unlike the chains of a playground swing. (see appendix 8.9)
2. Furthering the previous assumption, the pivots the rods rotate about are frictionless. (see section 4.1)
3. In deriving the solution trajectory near critical points, the small angle approximation is used i.e. sin(θ) = θ.
4. The mass of the swing, person, and rods are approximated by a point mass at the position of the combined center of mass of the system.

6.1 Simple Harmonic Pendulum

Applying `solve_ivp` to the differential equation 5.3 using sensible initial conditions: $\theta(t = 0) = 0.244$ rad, $\dot{\theta}(t = 0) = 0$ we can recreate the motion of a simple pendulum undergoing simple harmonic motion. A plot showing this motion in the x-y plane can be seen in figure 5.

6.2 Anharmonic Motion with Fixed Length

Figure 6 illustrates the behaviour of $\frac{du}{d\theta} = \frac{-\omega_0^2 sin(\theta)}{\theta}$ for $t \geq 0$, where $\omega_0^2 = \frac{g}{l}$. The null clines are given by the sets of curves where $\frac{d\theta}{dt} = 0$ and $\frac{du}{dt} = 0$, i.e. $\frac{du}{d\theta} = \infty$ and 0 respectively. In this case, $\lambda_{1/2}$ are a complex conjugate pair for n even with vanishing real component, hence (0, 0) is a centre with an uncertain stability. For n odd, $\lambda_{1/2}$ are real and $\lambda_1 \leq 0 < \lambda_2$, so the points (0, +/-3) are unstable saddle points that wouldn't be observed in the real behaviour of the swing. The plot repeats every $\theta = 2x\pi$ where x is an integer, this is because the pendulum is in the same physical position for every θ and $\theta + 2\pi$.

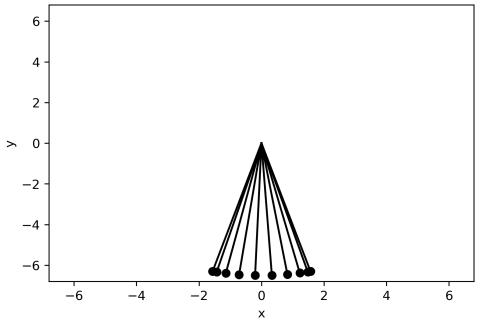

Figure 5: Motion of a simple pendulum undergoing simple harmonic motion in the x-y plane with initial angle 0.244 rad

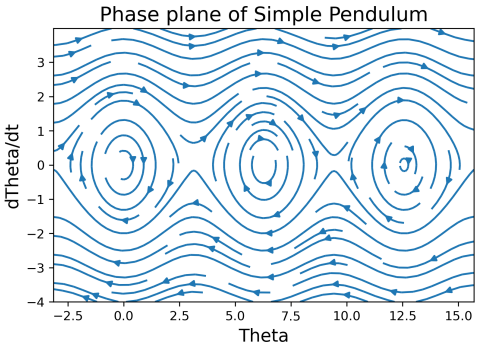

Figure 6: A plot of the solution trajectory for a swing without damping forces

Figure 7 illustrates the behaviour of $\frac{du}{d\theta} = \frac{-(u\gamma + \omega_0^2 \sin(\theta))}{\theta}$ for $t \geq 0$, where $\gamma = \frac{C}{l}$ is the damping constant and is equal to 0.3 s^{-1} in our analysis. The two sets of null clines where $\frac{du}{d\theta} = 0$ or ∞ are shown. In this case, $\lambda_{1/2}$ are a complex conjugate pair for n even assuming $\gamma < 2\omega$ with a negative real component, hence the point (0, 0) is a stable spiral. Following the same reasoning as in the zero-damping case, the

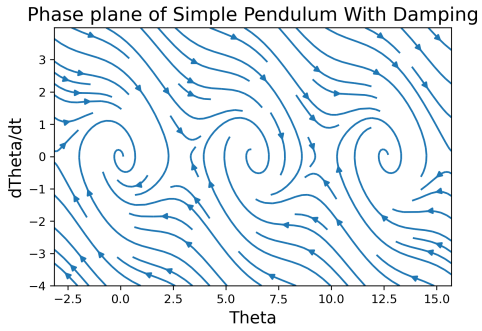

Figure 7: A plot of the solution trajectory for a swing with damping forces of 0.5 s^{-1}

points (0, +/-3) are unstable saddle points that wouldn't be observed in the motion of a real swing.

6.3 Anharmonic

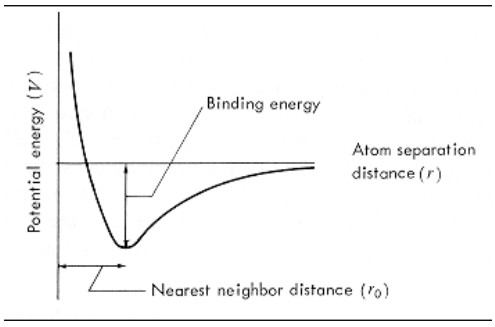

Figure 8: Motion of a pumped swing in the x-y plane with initial angle 0.244 rad, it is clear to see the change in length of the swing arm indicating the change in centre of mass produced by pumping

Again applying `solve_ivp`, this time to solve equation 5.26 we are able to resolve the motion of a pumped swing in the x-y plane. This motion can be seen in figure 8, here we can see the change in centre of mass as a result of pumping. Figure 8 only shows the motion of the swing over the initial period, by increasing how long we let the model run for we can see the motion over several periods. Illustrated in Figure 9 we can see the maximum angle θ achieved over different time frames. This showcases how the pump motion increases the max θ and can eventually be used to complete a full 360°. Through steadily increasing the time frame of the model we can accurately predict

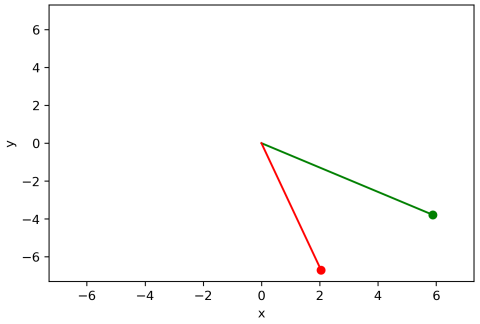

Figure 9: Plot illustrating the maximum angle θ achieved after 15s of pumping (red) and after 100s of pumping (green)

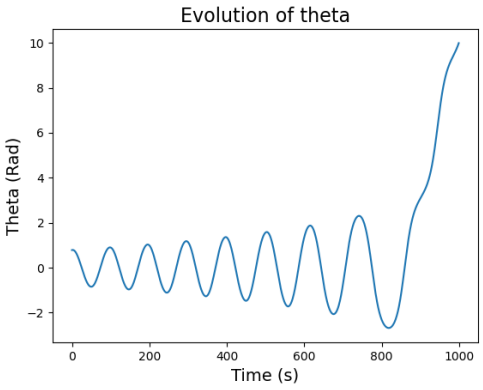

Figure 10: Time evolution of theta under damping forces and with pumping at $\theta = 0$

when the initial 360° will occur. We can choose values to input to the model that correspond to the world record for the longest swing shaft used to successfully complete a full rotation [16]. For a mass of 96 kg, a swing arm length of 7.38 m (when crouched) and assuming a difference in crouched vs standing of 1 m, the first full rotation will be possible after 84 s or 14 full periods. This is of course assuming impossibly perfect pumping technique where the crouch/stand up happens instantaneously, for a genuine human competitor this will be harder to achieve and will take more time/periods, however the value stated is the theoretical earliest possible moment that a full rotation could happen.

Figure 10 illustrates how the angular displacement of the point mass evolves as pumping occurs at the point of zero angular displacement under damping torque. At around t = 800s the angular displacement of the point mass is large

enough that it's angular velocity at $\theta = 0$ is sufficient for it remain greater than zero while it pivots about the fulcrum, completing one full rotation. It should also be noted as each swing gets closer to completing a full revolution, the period of the last few swings increases. This behaviour is expected based on the phase plane transition from a centre to unstable, as the swing spends more time at low velocity at the top of each swing, where θ is marginally below 2π.

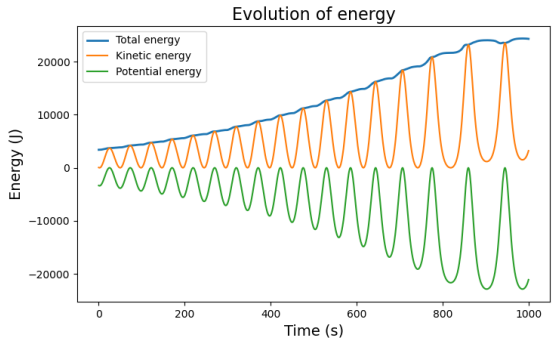

Figure 11: Time evolution of the total energy of the system under damping forces and with pumping at $\theta = 0$

Figure 13 illustrates how the kinetic, potential and total energy (kinetic + potential) of the system evolve with time under damping and pumping. The peak kinetic energy of the point mass (which occurs at $\theta = 0$) increases with each cycle, while the maximum potential energy (which occurs at $\theta = \theta_{max}$ where $\omega = 0$) also increases each cycle, indicating that pumping is effective at increasing the maximum amplitude of the swing with each cycle. From equation 8.9 it is clear that in order to produce a large change in the angular momentum of the system, it is important that the person has a greater centre of mass and also is able to move their centre of mass through a longer distance as quickly as possible. For these reasons, a heavier, taller and more physically fit competitor (assuming they also have skill) will have a significant advantage compared with other competitors to complete one full rotation in the shortest time.

7 Conclusion

In this paper, both Simple Harmonic motion and Anharmonic motion were modelled to simulate a Kiiking swing.

In the case of SHM, the motion of a simple pendulum without damping was resolved both in the x-y and phase plane with an initial angle of 0.244 rad and an initial angular-velocity of $\omega = \sqrt{\frac{g}{l}} = 1.15$ rad s^{-1}. As could be anticipated, the solution trajectory repeated every 2π radians, where for even n $\lambda_{1/2}$ were complex with vanishing real component and hence critical points at angular displacements of even multiples of π were centres with uncertain stability. At angular displacements of odd multiples of pi, we found unstable saddle points. When damping was considered, setting $\gamma = \frac{C}{l} = 0.3$ s^{-1}, we discovered that critical points at angular displacements of even multiples of pi were stable spirals. Similar to the non-damped case, angular displacements of odd multiples of π led to the formation of unstable saddle points.

In the Anharmonic case, the center of mass of the pendulum was changed during each period to simulate the pumping motion of Kiiking. Using a mass of 96 kg and a swing arm length of 7.38 m when squatting and 6.38 m when standing, the first full rotation occurred after 84 s or 14 full periods. The Energy of the system was also evaluated, which indicated that the peak kinetic and potential energy of the point mass (occurring at $\theta = 0$ and $\theta = \theta_{max}$ respectively) increased with each cycle. From this, it was concluded that pumping is effective at increasing the maximum amplitude of motion. We also noted that in order to complete a full rotation in the shortest amount of time, the competitor should be tall and heavy with good physical fitness such that they can produce a larger change in the angular momentum of the system compared with other competitors.

8 Appendix

8.1 Newton's Second Law

A particle acted upon by a resultant force moves so that the rate of change for a single particle.

$$\sum \underline{F} = m\underline{a} \tag{8.1}$$

For a single particle, where $\sum \underline{F}$ is the resultant force, m is the mass, and $\underline{a}$ is the acceleration.

8.1.1 Remark from Newton's Second Law

Newton's Second Law implies the requirement for an inertial frame of reference because $\frac{dp}{dt}$ depends on a reference frame which is the direction motion is observed. The need for a reference frame is not the case for the particle's mass or the forces applied to the particle.

8.2 Newton's Second Law for a Cartesian 2D-Coordinate System

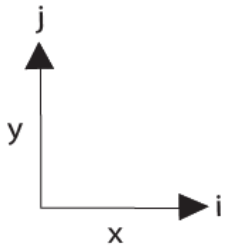

Figure 12: 2d Cartesian Coordinate System

$$\underline{r} = \underline{x}\hat{i} + \underline{y}\hat{j} \tag{8.2}$$

The velocity of a particle A is the rate of change of it's position. $\underline{r}$ is the position vector, t is the time. The direction of $\underline{v}$ is in the direction of $\Delta\underline{r}$ as $\Delta t \to 0$.

$$\underline{v} = \lim_{\Delta t \to 0} \frac{\Delta \underline{r}}{\Delta t} \tag{8.3}$$

$$\underline{v} = \dot{\underline{r}} = \dot{\underline{x}}\hat{i} + \dot{\underline{y}}\hat{j} \tag{8.4}$$

The acceleration is the rate of change of it's velocity.

$$\underline{a} = \frac{d\underline{v}}{dt} = \frac{d^2\underline{r}}{dt^2} \tag{8.5}$$

$$\underline{a} = \dot{\underline{v}} = \ddot{\underline{r}} = \ddot{\underline{x}}\hat{i} + \ddot{\underline{y}}\hat{j} \tag{8.6}$$

Combined, We have,

$$\sum \underline{F} = m\underline{a} = m\frac{d^2\underline{r}}{dt^2} \tag{8.7}$$

8.3 The Principle Of Linear Momentum

$$\sum \underline{F} = \frac{\mathrm{d}(m\underline{v})}{\mathrm{d}t} = \dot{p} \tag{8.8}$$

Where $p = m\underline{v}$ is the linear momentum of a particle. if $\sum \underline{F} = \underline{0}$, the value of p is constant and the linear momentum is conserved.

8.4 The Principle Of Angular Momentum

Here, we define point A's angular momentum in an inertial frame of reference.

$$\underline{h_A} = \underline{r} \times m\underline{v} \tag{8.9}$$

$\underline{h_A}$ is the moment of linear momentum about the point A.

8.4.1 Conservation of Angular Momentum

Taking time derivatives of 23 we can investigate properties of the moment of linear momentum.

$$\frac{\mathrm{d}\underline{h_A}}{\mathrm{d}t} = \dot{\underline{r}} \times m\underline{v} + \underline{r} \times m\dot{\underline{v}} \tag{8.10}$$

The vector $\underline{r}$ is a vector defined as the distance between the position $\underline{R_A}$ and the new position $\underline{R}$.

$$\frac{\mathrm{d}\underline{h_A}}{\mathrm{d}t} = (\dot{\underline{R}} - \dot{\underline{R}_A}) \times m\underline{v} + \underline{r} \times \sum \underline{F} \tag{8.11}$$

Using that, $\dot{\underline{R}} = \underline{v}$ and $\dot{\underline{R}_A} = \underline{v_A}$

$$\frac{\mathrm{d}\underline{h_A}}{\mathrm{d}t} = (\underline{v} \times m\underline{v}) - \underline{v_A} \times m\underline{v} + \underline{r} \times \sum \underline{F} \tag{8.12}$$

$\underline{v} \times m\underline{v} = 0$, because its the cross product of two parallel vectors.

$$\frac{\mathrm{d}\underline{h}_A}{\mathrm{d}t} = \dot{\underline{h}_A} = -\underline{v}_A \times m\underline{v} + \underline{r} \times \sum \underline{F} \tag{8.13}$$

Define the resultant torque as $\underline{\tau}_A = \underline{r} \times \sum F$ and combine with equation (27). This yields the result:

$$\underline{\tau}_A = \dot{\underline{h}_A} + v_A \times m\underline{v} \tag{8.14}$$

if $\underline{\tau}_A = 0$ and $v_A = 0$ or v_A is parallel to $m\underline{v}$. This implies that $\dot{\underline{h}_A} = 0$ and $\underline{h}_A$ is a *constant* and the angular momentum is conserved.

8.5 Calculation of Eigenvalues from equation 5.13

$$\begin{pmatrix} \hat{x} \\ \hat{y} \end{pmatrix}' = \begin{pmatrix} 0 & 1 \\ -\omega^2 & 0 \end{pmatrix} \begin{pmatrix} \hat{x} \\ \hat{y} \end{pmatrix} \tag{8.15}$$

$$B = \begin{pmatrix} -\lambda & 1 \\ -\omega^2 & -\lambda \end{pmatrix} \tag{8.16}$$

$$\begin{aligned} det(B) = \lambda^2 + \omega^2 = 0 \\ \lambda^2 = -\omega^2 \\ \lambda_\pm = \pm\omega i \end{aligned} \tag{8.17}$$

8.6 Calculation of Eigenvalues and Eigenvectors from Equation 5.17

$$\begin{pmatrix} \hat{x} \\ \hat{y} \end{pmatrix}' = \begin{pmatrix} 0 & 1 \\ \omega^2 & 0 \end{pmatrix} \begin{pmatrix} \hat{x} \\ \hat{y} \end{pmatrix} \tag{8.18}$$

$$B = \begin{pmatrix} -\lambda & 1 \\ \omega^2 & -\lambda \end{pmatrix} \tag{8.19}$$

$$\begin{aligned} det(B) = \lambda^2 - \omega^2 = 0 \\ \lambda^2 = \omega^2 \\ \lambda_\pm = \pm\omega \end{aligned} \tag{8.20}$$

For λ = ω:

$$\begin{pmatrix} 0 & 1 \\ \omega^2 & 0 \end{pmatrix} \begin{pmatrix} x \\ y \end{pmatrix} = \omega \begin{pmatrix} x \\ y \end{pmatrix} \tag{8.21}$$

$$\begin{pmatrix} y \\ \omega^2 x \end{pmatrix} = \begin{pmatrix} \omega x \\ \omega y \end{pmatrix} \tag{8.22}$$

Here we have $y = \omega x$. Let, $x = 1$. Then We have $(1, \omega)^T$ as our eigenvector for $\lambda = \omega$.

For λ = -ω:

$$\begin{pmatrix} 0 & 1 \\ \omega^2 & 0 \end{pmatrix} \begin{pmatrix} x \\ y \end{pmatrix} = -\omega \begin{pmatrix} x \\ y \end{pmatrix} \tag{8.23}$$

$$\begin{pmatrix} y \\ \omega^2 x \end{pmatrix} = \begin{pmatrix} -\omega x \\ -\omega y \end{pmatrix} \tag{8.24}$$

Here we have $y = -\omega x$. Let, $x = 1$. Then We have $(1, -\omega)^T$ as our eigenvector for $\lambda = -\omega$.

8.7 Calculation of Eigenvalues from Equation 5.19

$$\begin{pmatrix} x \\ y \end{pmatrix}' = \begin{pmatrix} 0 & 1 \\ -\omega^2 & -\gamma \end{pmatrix} \begin{pmatrix} x \\ y \end{pmatrix} \tag{8.25}$$

$$\begin{pmatrix} -\lambda & 1 \\ -\omega^2 - \gamma & -\lambda \end{pmatrix} \tag{8.26}$$

$$\begin{aligned} (\gamma + \lambda)(\lambda) - (-\omega^2) \\ \lambda^2 + \gamma\lambda + \omega^2 = 0 \end{aligned} \tag{8.27}$$

$$\lambda_\pm = \frac{-\lambda \pm \sqrt{\gamma^2 - 4 \cdot 1 \cdot \omega^2}}{2} \tag{8.28}$$

Assume $\gamma^2 < 4 \cdot \omega^2$

$$\begin{aligned} \lambda_\pm = \frac{-\gamma \pm i\sqrt{\gamma^2 - 4\omega^2}}{2} \\ \lambda_\pm = -\frac{\gamma}{2} \pm i\sqrt{\omega^2 - \frac{\gamma^2}{4}} \end{aligned} \tag{8.29}$$

8.7.1 Calculation of Eigenvalues from Equation 5.20

$$\begin{pmatrix} x \\ y \end{pmatrix}' = \begin{pmatrix} 0 & 1 \\ \omega^2 & -\gamma \end{pmatrix} \begin{pmatrix} x \\ y \end{pmatrix} \tag{8.30}$$

$$\begin{pmatrix} -\lambda & 1 \\ \omega^2 - \gamma & -\lambda \end{pmatrix} \tag{8.31}$$

$$\lambda^2 + \gamma\lambda - \omega^2 = 0 \tag{8.32}$$

$$\lambda_{\pm} = \frac{-\gamma \pm \sqrt{\gamma^2 + 4\omega^2}}{2} \tag{8.33}$$

Assuming $\gamma^2 > 4\omega^2$

$$\lambda_{\pm} = -\frac{\gamma}{2} \pm \sqrt{\omega^2 + \frac{\gamma^2}{4}} \tag{8.34}$$

8.8 Euler Approximation

The Runge-Kutta Method is found using the Euler method. An initial value problem in form (eqn) is solved.

$$y' = f(x,y), y(x_0) = y_0 \tag{8.35}$$

By introducing a small step h the first estimate can be approximated as:

$$y(x_1) \equiv y(x_0 + h) \tag{8.36}$$

This is expanded using Taylor's Theorem as follows:

$$y(x_1) = y(x_0) + y'(x_0)h + \mathcal{O}(h^2) \tag{8.37}$$

$$y(x_1) = y(x_0) + hf(x_0, y(x_0)) + \mathcal{O}(h^2) \tag{8.38}$$

Further approximations, y_{n+1}, are obtained as:

$$y_{n+1} \equiv y(x_{n+1}) = y_n + hf(x_n, y_n) + \mathcal{O}(h^2) \tag{8.39}$$

Euler's method's precision and reliability rests on making h small, however, due to the inaccurate and potential unstable nature of this method, it is only useful for differential equations that converge quickly. This method can be improved using the predictor-corrector method which produces 3rd order local error, and 2nd order global error [4] [2]. Without the predictor-corrector method to estimate an average of the slope, the Euler method has a large truncation error as the derivatives are calculated at the start of the interval which causes asymmetry [5].

8.9 Extensible supports

In the sport of Kiiking, the rods attaching the swing to the pivot are (to a very good approximation) inextensible and rigid, being that they are made of alloy steel [15]. However, we can explore the possibility of the rods being composed of an extensible, non-rigid material like in a playground swing. In this case, one could treat the swing-human-rod system as an N-pendulum, i.e. a series of N coupled pendulums initially aligned along e_r. Moreover, if we discrete the mass distribution into N point masses:

$$M_{TOT} = \Sigma_{k=1}^{N} dm_k \tag{8.40}$$

Then the behaviour of the system of N coupled pendulums is described by the following equation, derived using Lagrangian mechanics:

$$\begin{aligned} &\Sigma_{k=1}^{N}(g l_j sin(\theta_j) m_k \sigma_{jk} + m_k l_j^2 \ddot{\theta}_j \sigma_{jk} \\ &+(\Sigma_{q\geq k}^{N} * m_q \sigma_{jq}) l_k l_j sin(\theta_j - \theta_k)\dot{\theta}_j \dot{\theta_K} \\ &+(\Sigma_{q\geq k}^{N} * m_q \sigma_{jq}) l_j l_k [\sin(\theta_k - \theta_j)] \\ &(\dot{\theta}_j - \dot{\theta}_k) = 0 \end{aligned} \tag{8.41}$$

Where σ_{jk} is 0 if $j > k$ and 1 if $j \leq k$ [13]. Solving this using RK4 or a similar numerical integration technique would produce an approximate solution in the scenario that the supports are extensible, although this would be extremely computationally demanding for large N.

8.10 Polar co-ordinate derivation for varied r(t)

We introduce a time-varying pendulum length $r(t)$ where:

$$\mathbf{r}(t) = r(t)\mathbf{e}_r \tag{8.42}$$

Here $\mathbf{e}_r$ is the radial unit vector, and $\mathbf{e}_\theta$ is the unit vector in the direction of motion of the point mass and is perpendicular to $\mathbf{e}_r$ (see figure **??**). They are defined in terms of the cartesian unit vectors $\mathbf{e}_x$ and $\mathbf{e}_y$ by:

$$\mathbf{e}_r = \cos\theta \mathbf{e}_x + \sin\theta \mathbf{e}_y \tag{8.43}$$

$$\mathbf{e}_\theta = -\sin\theta \mathbf{e}_x + \cos\theta \mathbf{e}_y \tag{8.44}$$

Therefore the Cartesian unit vectors in terms of the polar unit vectors are:

$$\mathbf{e}_x = \cos\theta \mathbf{e}_r - \sin\theta \mathbf{e}_\theta \tag{8.45}$$

$$\mathbf{e}_y = \sin\theta \mathbf{e}_r + \cos\theta \mathbf{e}_\theta \tag{8.46}$$

We can use equations 8.43 and 8.44 to obtain expressions for the derivatives of $\mathbf{e}_r$ and $\mathbf{e}_\theta$:

$$\frac{d}{dt}\mathbf{e}_r = \frac{d\theta}{dt}(-\sin\theta \mathbf{e}_x + \cos\theta \mathbf{e}_y) = \frac{d\theta}{dt}\mathbf{e}_\theta \tag{8.47}$$

$$\frac{d}{dt}\mathbf{e}_\theta = \frac{d\theta}{dt}(-\cos\theta \mathbf{e}_x - \sin\theta \mathbf{e}_y) = -\frac{d\theta}{dt}\mathbf{e}_r \tag{8.48}$$

The total force on a pendulum with mass m is made up of a gravitational force mg in the positive x-direction (downwards), and a tension force T in the negative r-direction (upwards along the pendulum, figure **??**):

$$F = mg\mathbf{e}_x - T\mathbf{e}_r \tag{8.49}$$

Using Newton's 2nd Law $F = ma$ then allows us to write down an expression for its vector law of motion

$$m\frac{d^2r}{dt^2} = mg\mathbf{e}_x - T\mathbf{e}_r \tag{8.50}$$

It follows from equation 8.43, the definition of r, and the equations for the derivatives of the basis vectors (8.47,8.48) that

$$\begin{aligned} \frac{dr}{dt} &= \dot{r}(t)\mathbf{e}_r + r\dot{\theta}(t)\mathbf{e}_\theta \\ \implies \frac{d^2r}{dt^2} &= \left(\ddot{r} - r\dot{\theta}^2\right)\mathbf{e}_r + (2\dot{r}\dot{\theta} + r\ddot{\theta})\mathbf{e}_\theta \end{aligned} \tag{8.51}$$

If we now substitute equation 8.51 into the polar form of Newton's 2nd Law equation 8.50, and divide through by m, we obtain the following vector equation:

$$\begin{aligned} \left(r - r\dot{\theta}^2\right)\mathbf{e}_r + (2\dot{r}\dot{\theta} + r\ddot{\theta})\mathbf{e}_\theta = \\ g(\cos\theta \mathbf{e}_r - \sin\theta \mathbf{e}_\theta) - \frac{T}{m}\mathbf{e}_r \end{aligned} \tag{8.52}$$

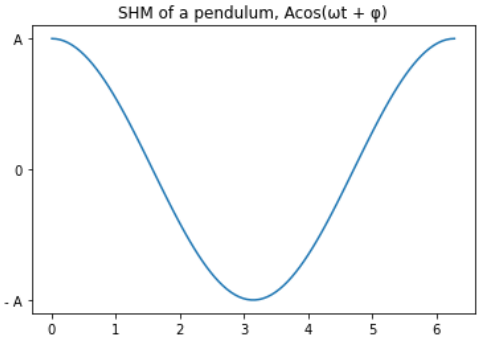

Figure 13: Simple Harmonic Motion of a pendulum for $\phi = 0$.

References

Wirkus, Stephen, et al. "The College Mathematics Journal" Vol. 29, No. 4. Mathematical Association of America, Sept. 1998.

Hawke, Ian. "MATH3018 MATH6141 Numerical Methods. University of Southampton", 2017.

BUTCHER, J. C. "Practical Runge-Kutta Methods for Scientific Computation." The ANZIAM Journal, vol. 50, no. 3, Jan. 2009.

Liengme, Bernard V. "SMath for Physics" Iopscience.iop.org, 2015.

"Runge-Kutta Methods.", University of Texas, Farside.ph.utexas.edu.

Bhopale, Mahananda. "Review Paper on the Applications of Runge- Kutta Method to Solve the Differential Equations." No. 6, 2019.

Greulich, Phillip, et al. "MATH3052 Mathematical Biology. University of Southampton", 2020.

Moghimi-Araghi, S. and Loran, F. "Anharmonic oscillator: A playground to get insight into renormalization. European Journal of Physics", 2021.

Peacock, T. "2.003J/1.053J Dynamics and Control I, Massachusetts Institute of Technology", 2007.

Fenz, D. M., 2006. Behaviour of the double concave Friction Pendulum bearing. Wiley Online Library.

Hinrichsen, P., 2014. Pendulum Bearing Friction. ResearchGate

Engineering ToolBox, (2004). Friction - Friction Coefficients and Calculator. Available at: https://www.engineeringtoolbox.com/friction-coefficients-d_778.html

Yesilyurt, B., 2019. Equation of motion formuation of a pendulum containing N point masses. ResearchGate

Bradshaw, Luke (17 November 2017). "Estonia and its Love for Extreme Swinging". Culture Trip.

Vissel, Anu (2002). "Eestlaste kiigekultuur enne ja nüüd" (PDF). Mäetagused (in Estonian). 21: 7–84. doi:10.7592/MT2002.21.kiik

"Longest successful 360° kiiking swing (male)". Guinness World Records. Retrieved 26 August 2021

9 Individual contributions

1. Matt - Coding of Model (SHM, Anharmonic with variable r(t) no damping), Derivation of the pumping function (section 5.4.1), contributed to results and discussion in sections 6.1 and 6.3

2. Delice - Provided Numerical Solutions to ODEs in **Motivational Model**, **Model I** and **Model II** ; Provided the theory and mathematical deviation of N2L in 2D Cartesian Coordinates ; Contributed to the writing of Sections 3, 5.1, 5.2, 5.3.

3. Jacinta - Sections 2.1, 6.0, 7, 8.8 (appendix). Wrote up and formatted the derivations in sections 3, 5, 8.1 - 8.7, 8.10.

4. Ollie - Abstract, Introduction, Derivation of Anharmonic System with $r(t)$ using Polar Coordinates (Sections 5.4, 8.10)

5. Aakash - Coding of Model; finding solutions to ODEs in the **Motivational Model**, **Model I** and **Model II**. Constructed Phase Plane, Evolution of Theta and Evolution of Energy graphs. Also contributed to Theory in section 3 and discussion of results in section 6.3.

6. Ralph - Section 4, 2.2, 6.2 and 8.9 (appendix). Contributed to sections 6.3 and 7.